Formulation of Performance Levels and Relevant Limitations for Clay Brick Masonry Infills in Seismic Analysis of R/C Frame Structures

Formulation of Performance Levels and Relevant Limitations for Clay Brick Masonry Infills in Seismic Analysis of R/C Frame Structures

Iacopo Costoli [1], Stefano Sorace [1], Gloria Terenzi [2]

[1] Polytechnic Department of Engineering and Architecture, University of Udine, 33100 Udine, Italy
[2] Department of Civil Environmental Engineering, University of Florence, 50139 Florence, Italy

iacopo.costoli@uniud.it

Abstract. Observation of damage caused by recent earthquakes highlights, once again, that the presence of infills significantly affects the seismic response of reinforced concrete (R.C.) frame buildings. Therefore, in spite of the fact that infills are non-structural elements, and thus they are normally not considered in structural analyses, in many cases their contribution should not be neglected. Based on these observations, the study proposed in this paper consists in the evaluation of the seismic response of infills in time-history finite element analyses of R.C. frame structures by means of a two-element model, constituted by two diagonal nonlinear beams. A “concrete”-type hysteretic model predicts the in-plane state of infills, through a force-displacement backbone curve expressly generated, and scanned in terms of performance limits, to this aim. This model is demonstratively applied to a real case study, i.e. a R.C. frame building including various types of brick masonry perimeter infills and internal partitions, damaged by the 30 October 2016 Central Italy earthquake. The time-histories seismic analyses carried out on it allows checking the influence of infills on the response of the structure, as well the effectiveness of the proposed model in reproducing the observed real damage on the masonry panels.

1. Introduction

As is known, the seismic response of reinforced concrete (R.C.) structures is considerably influenced by their interaction with masonry infill panels built in contact with the frame members. This is also recognized by the Italian Seismic Standards [1], as well as by Eurocode 8 [2], where the Operational (OP) and Immediate Occupancy (IO) performance levels are expressly referred to the evaluation of damage in infills. However, whereas the limit values of the inter-storey drift ratio are fixed in these Standards as quantitative assessment criteria for both levels, no suggestions on the evaluation of damage evolution in infills, from the beginning of cracks up to collapse, are provided.

In view of this, a study is proposed in this paper, aimed at assessing the response of brick masonry infills in time-history finite element analyses, by relating their lateral displacements to expressly formulated performance levels. The behaviour of infills is simulated by means of a two-element model, constituted by two diagonal no-tension nonlinear beams. A force-displacement “backbone” curve is expressly built to describe their in-plane response, governed by a hysteretic "concrete"-type

model. This model is demonstratively applied to a real R.C. frame building including various types of perimeter infills and internal partitions, most of which were severely damaged by the Central Italy earthquake of 30 October 2016.

2. Infill model description

The numerical model simulates the typical seismic response of infills during the seismic response of the R.C. structure where they are incorporated, i.e.: at the beginning, the undamaged infills interact with the frame members absorbing a portion of the horizontal action by means of their shear stiffness; then, as seismic action increases, the panels tend to detach from the R.C. members along their span (beams) and height (columns), offering a residual collaboration to the dynamic response of the structure in the form of equivalent compressed diagonal struts converging to the centre of the beam-to-column joints.

The behaviour of the equivalent struts is schematically described by the σ-ε stress-strain cyclic response curves and relevant peak envelope illustrated in Figure 1.a and 1.b, respectively [3].

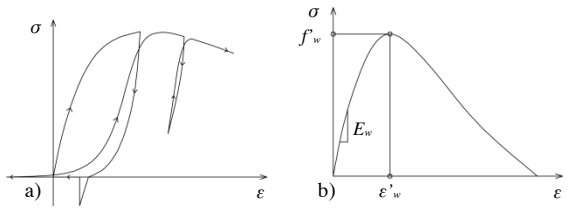

Figure 1. a) Stress-strain cyclic response of the equivalent strut model; b) envelope of relevant peak values (adapted from [3])

The equivalent strut length of panels is obtained by the following relation [4]:

$$b_w = \left(\frac{K_1}{\lambda h} + K_2\right) d_w \tag{1}$$

where: d_w = length of the compressed strut, λh = dimensional parameter [5], function of the geometric and mechanical characteristics of the system, K_1, K_2 = empirical coefficients, depending on the value of λh, as specified in Table 1.

Table 1. K_1 and K_2 coefficient values

	$\lambda h < 3.14$	$3.14 < \lambda h < 7.85$	$\lambda h < 7.85$
K_1	1.3	0.707	0.47
K_2	-0.178	0.01	0.04

The λh parameter is a measure of the stiffness of the infilled frame, where λ is defined as follows [6]:

$$\lambda = \sqrt[4]{\frac{E_{w\emptyset}\, t_w\, sin2\emptyset}{4E_c\, I_c\, h_w}} \tag{2}$$

being: h_w, t_w = height and thickness of the infill panel, E_c = modulus of elasticity of the material constituting the columns of the frame structure (concrete, in the case of R.C. structures), I_c = moment of inertia of the infilled frame along the axis orthogonal to the horizontal load direction, ϑ =

inclination angle of the compressed strut, and $E_{w\emptyset}$ = elastic modulus of the material constituting the infills, calculated in the direction parallel to the compressed strut, given by:

$$E_{w\emptyset} = \left[\frac{cos^4\,\emptyset}{E_{wh}} + \frac{sin^4\,\emptyset}{E_{wv}} + cos^2\emptyset + sin^2\emptyset\left(\frac{1}{G} - \frac{\nu}{E_{wh}}\right)\right]^{-1} \quad (3)$$

where ν is the Poisson ratio, and E_{wh}, E_{wv} G are the horizontal elastic modulus, the vertical elastic modulus and the shear modulus of the panel, respectively.

The strength values of the masonry panels are obtained by referring to the classical expression [4]:

$$F_w = \sigma_{w,min}\, b_w\, t_w\, cos\emptyset \quad (4)$$

where $\sigma_{w,min}$ is the minimum stress value associated to the achievement of one of the four possible crisis mechanisms of the infill panel (Figure 2), that is, caused by compression in the middle (σ_{w1}), compression at the corners (σ_{w2}), shear-sliding (σ_{w3}), and shear-diagonal crack (σ_{w4}), which are evaluated as follows:

$$\sigma_{w1} = \frac{1.16\, f_{wv}\, tan\emptyset}{K_1 + K_2\, \lambda h} \quad (5)$$

$$\sigma_{w2} = \frac{1.12\, f_{wv}\, sin\emptyset\, cos\emptyset}{K_1(\lambda h)^{-0.12} + K_2(\lambda h)^{0.88}} \quad (6)$$

$$\sigma_{w3} = \frac{(1.12\, sin\emptyset + 0.45\, cos\emptyset) f_{wv} + 0.3\, \sigma_v}{b_w/d_w} \quad (7)$$

$$\sigma_{w4} = \frac{0.6\, sin\emptyset\, f_{ws} + 0.3\, \sigma_v}{b_w/d_w} \quad (8)$$

.

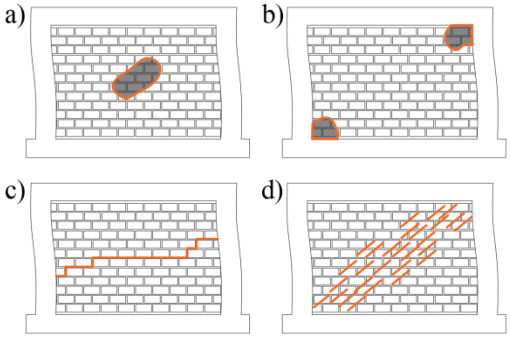

Figure 2. Crisis mechanism of the infill panels: a) compression in the middle; b) compression at the corners; c) shear-sliding; d) shear-diagonal crack

In expressions (5) through (8) f_{wv} is the compressive strength of the panel, f_{wu} and f_{ws} the shear strength of the joints and referred to diagonal cracking, respectively, whereas σ_v is the compression stress, null for panels without load-bearing function with respect to vertical loads. The F-Δ force-drift ratio (i.e. the ratio of inter-storey drift to inter-storey height, h_m) backbone curve of the "concrete"-type no-tension multilinear plastic element adopted for the simulation of the behaviour of masonry infills in finite element analyses is shown in Figure 3.

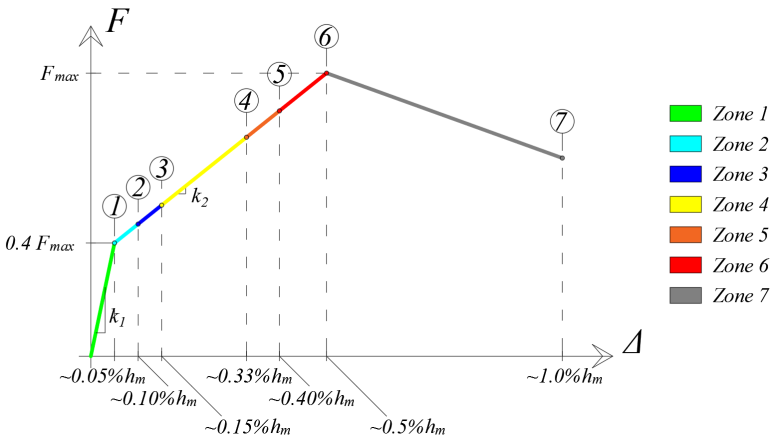

Figure 3. Backbone curve of the "concrete-type" multilinear plastic element adopted for finite element analyses the masonry infills

The backbone curve was characterized in this study by means of the seven performance points, recapitulated below.

Point 1 represents the conclusion of the first response branch, corresponding to a non-cracked linear-elastic behaviour of the panel (fixed at $\Delta = 0.05\%$). A first set of nearly invisible cracks starts from point 1, causing a loss of stiffness. Points 2 ($\Delta = 0.1\%$) and 3 ($\Delta = 0.15\%$) mark the beginning of a visible—2— and more appreciable—3—manifestation of superficial cracking. In depth cracking effects begin at point 4 ($\Delta = 0.33\%$), which is assumed by several Standards as the drift ratio limit identifying the building Operational performance level in the presence of masonry infills. Point 5 ($\Delta = 0.4\%$) corresponds to the first detachment of the lateral sides of the panel from the R.C. columns and the upper side from the beams. Point 6 ($\Delta = 0.5\%$) coincides with the attainment of the first appreciable level of damage triggering the subsequent development of the prevailing crisis mechanism. A softening branch follows point 6, up to point 7 (approximately fixed at $\Delta = 1\%$), where collapse is reached, as a result of the complete activation of the prevailing mechanism. The curve segments determined by the seven points are named Zone 1 through 7, and highlighted with a set of different colours, in Figure 3.

The k_1 and k_2 stiffness values characterizing the first and second ascending branches of the skeleton curve are computed as follows [4]:

$$k_1 = \frac{40 \cdot F_{max}}{0.05 \cdot h_w} \tag{9}$$

$$k_2 = \frac{60 \cdot F_{max}}{0.45 \cdot h_w} \tag{10}$$

3. Application to a case study building

The above-ground structural plan and longitudinal section of the case study building, situated in the municipality of Norcia, Umbria region (Italy), are presented in Figures 4 and 5, respectively. The structure is constituted by a R.C. frame system, integrated by a set of eight steel braces made of HEA 200 profiles in the central longitudinal alignment of the basement.

Figure 6 shows nomenclature and locations of the perimeter and internal clay brick masonry infills on the three above-ground storeys. According with this nomenclature, Tr1 represents double-layer (120 mm-thick solid brick internal + 80 mm-thick vertically hollowed external) perimeter walls without openings; Tr2 double-layer (120 mm-thick solid brick internal + 80 mm-thick vertically hollowed external) perimeter walls with openings; Tr3 double-layer (120 mm-thick solid brick internal + 80 mm-thick vertically hollowed external) main entrance lateral walls; Tr4 double-layer (80 mm + 80 mm-thick horizontally hollowed) internal partitions; Tr5 double-layer (80 mm + 80 mm-thick horizontally hollowed) staircase partitions; Tr6 single-layer (80 mm mm-thick horizontally hollowed) internal partitions; Lo1 double-layer (120 mm-thick solid brick internal + 80 mm-thick vertically hollowed external) perimeter walls with openings; Lo2 single-layer (80 mm mm-thick horizontally hollowed) internal partitions. The double-layer infill types have intermediate cavities between the constituting layers varying from 50 to 150 mm, depending on the specific locations in plan.

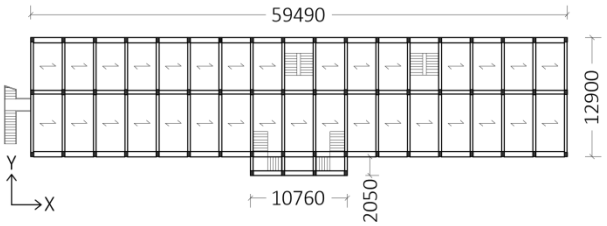

Figure 4. Structural plan of the above-ground storeys (dimensions in mm)

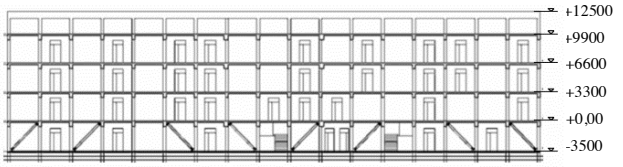

Figure 5. Longitudinal section of the building (dimensions in mm)

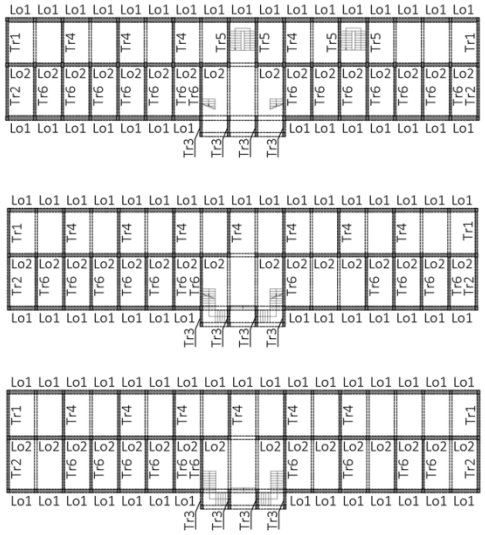

Figure 6. Nomenclature and locations of perimeter infills and internal partitions (from top to bottom plan: ground, first and second storey)

A time-history assessment analysis of the building was carried out by using the main shock ground motions of 30 October 2016 earthquake, recorded in Norcia seismographic station at 06:40:18, as input. The elastic pseudo-acceleration response spectra at linear viscous damping ratio $\xi = 5\%$ of the horizontal N-S and E-W component records, as well as of the vertical one, are plotted in Figure 7. The finite element model of the structure, a global view of which is displayed in Figure 8, was generated by the SAP2000NL calculus program (CSI 2020). Frame-type elements were assumed for the R/C columns and beams, and the model discussed above for perimeter infills and partitions.

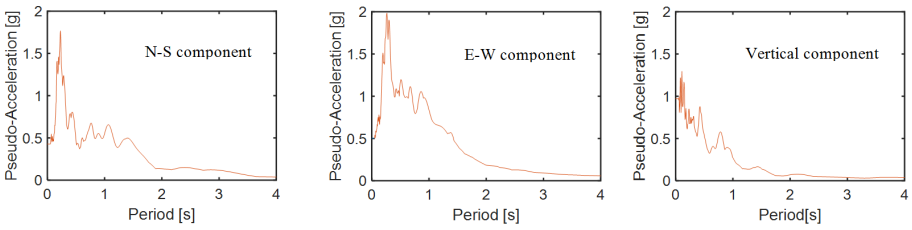

Figure 7. Pseudo-acceleration elastic response spectra of 06:40:18, 30 October 2016 Norcia seismograph records

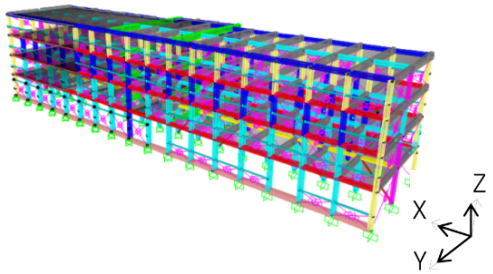

Figure 8. View of the finite element model of the structure

According with the planimetric layout of the building, the N-S component was basically introduced in input along Y axis and the E-W component along X (by referring to the Cartesian reference system drawn in Figure 8). For the sake of completeness, different orientations were also considered for the orthogonal components by varying their incidence angle in plan, which showed that the highest seismic demand was determined by the N-S parallel to Y and E-W parallel to X basic input motion orientation.

Based on the results of the time-history analysis, the stress state checks are not met by most structural members, with unsafety factors greater than 2 in the ground storey columns and beams, and significantly greater than 1 in the first and second storey ones.

The response of all infills and partitions belonging to the above-ground stories is beyond the cracking limit located by point 1, and for several panels it is situated in proximity to point 6, which corresponds to visible and not easy repairable crack-related damage. Moreover, all Lo2-type partitions cross point 6 and nearly reach collapse. In order to obtain a quick visual representation of the seismic performance of panels, their colour maps in X and Y direction referred to the colour scale in Figure 3 are plotted in Figures 9 and 10.

These results are in good agreement with the damage actually induced in the infills by the 30 October 2016 earthquake. By way of example, this is illustrated for Lo2-type partitions by the photographic images in Figure 11, taken during the immediate post-quake surveys, which highlight their shear-diagonal crack-associated near collapse conditions. The numerical response cycles of one

of these panels is plotted in Figure 12, which consistently shows the attainment of the descending branch of the backbone curve (Zone 7).

4. Conclusions

Based on analytical literature models simulating the in-plane response of masonry infills, and by combining the performance limits imposed by the reference Technical Standards with the results of selected experimental studies on this topic, a numerical macro-model constituted by two diagonal no-tension nonlinear beams was constructed, along with a backbone curve associated with a "concrete"-type hysteretic model.

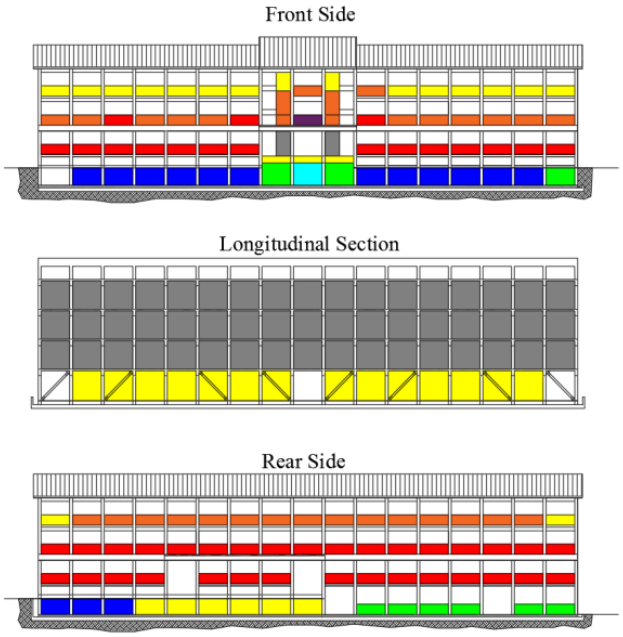

Figure 9. Colour maps assessing the response of perimeter infills and partitions of the building in X direction

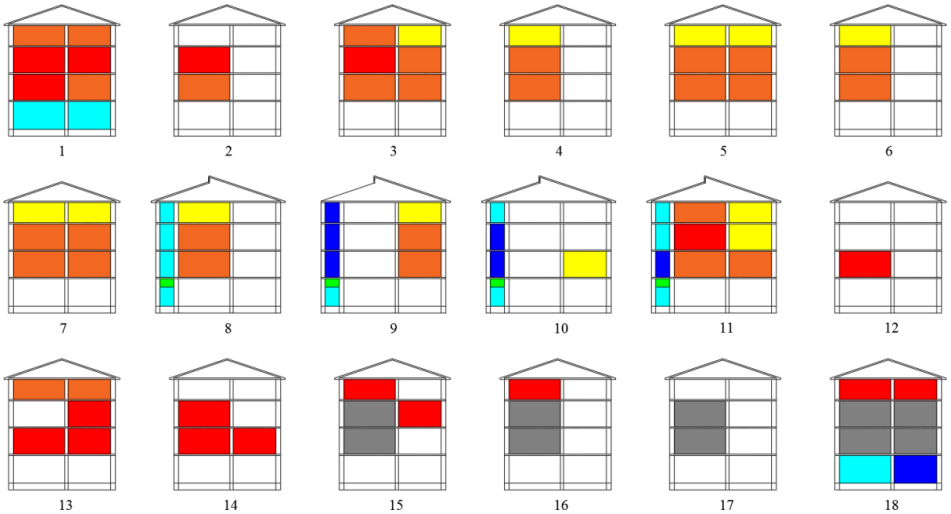

Figure 10. Colour maps assessing the response of perimeter infills and partitions of the building in Y direction

The curve was scanned by a series of characteristic response points, so as to evaluate the actual damage of the infills in intermediate states comprised between the attainment of the elastic limit and the in plane-collapse.

The application of the model to the finite element time-history analysis of a case study building hit by the Central Italy earthquake of 30 October 2016 allowed to observe a satisfactory correlation of the numerical results to the actual damage caused by this seismic event in the perimeter infills and the internal partitions.

Figure 11. Images of the ground storey Lo2-type longitudinal partitions taken after 30 October 2016 earthquake

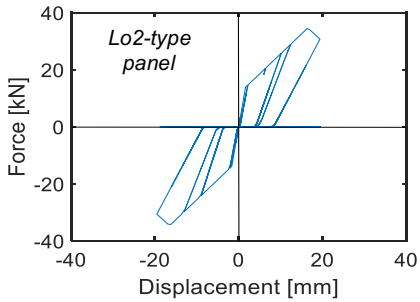

Figure 12. Response cycles of a first storey Lo2-type longitudinal partition panel

The definition of the performance points of the backbone skeleton curve needs further numerical validation studies, and an extension to the simulation of the out-of-plane response of the infill panels. Nonetheless, the feedback obtained at this stage of the research study clearly confirms the need for an explicit incorporation of infills in the finite element analysis of frame structures, both for the evaluation of seismic damage in the former and a more realistic assessment of the response of the latter, remarkably influenced by the mutual interaction of panels and structural members.

Acknowledgments
Financial support from ReLUIS-DPC Project 2019-2021 (WP 15: Normative Contributions for Isolation and Dissipation) is gratefully acknowledged.

References

[1] Ministerial Decree 17 January 2018, "Update of Technical Standards for Construction," Italian Ministry of Infrastructure and Transport, Rome, Italy, 2018 (in Italian).
[2] Eurocode 8, "Design of structures for earthquake resistance – Part 1: General rules, seismic actions and rules for buildings," The European Union, Directive 2004/18/EC, Brussels, Belgium, 2004.
[3] F. J. Crisafulli, "Seismic behaviour of reinforced concrete structures with masonry infills," PhD Thesis, University of Canterbury, Christchurch, New Zealand, 1997.

[4] S. H. Bertholdi, L. D. Decanini, and C. Gavarini, "Telai tamponati soggetti ad azione sismica, un modello semplificato: confronto sperimentale e numerico," *VI Italian National Conference on Earthquake Engineering*, 1993 (in Italian).
[5] B. Stafford Smith, "Behaviour of square infilled frames," *ASCE Journal of the Structural Division*, vol. 92(1), pp. 381–403, 1966.
[6] B. Stafford Smith, and C. Carter, "A method of analysis for infilled frames," *ICE Proceedings*, Paper No. 721, pp. 31–48, 1969.
[7] CSI, "SAP2000NL. Theoretical and user's manual. Release 22.03," Computers & Structures Inc., Berkeley, CA, USA, 2020.